Memorias del XVI Congreso Latinoamericano de Control Automático, CLCA 2014
Octubre 14-17, 2014. Cancún, Quintana Roo, México

Intelligent Classification of Heart Diseases Based on Radial Wavelet Neural Network

Juan E. Guillermo * Luis J. Ricalde Castellanos ** Edgar N. Sánchez * Braulio J. Cruz **

* *Automatic Control Departament, CINVESTAV of IPN, Guadalajara, Jalisco, México, (e-mail: jguillerm@gdl.cinvestav.mx, sanchez@gdl.cinvestav.mx)*
** *Faculty of Engineering, UADY, Mérida, Yucatán, México, (e-mail: lricalde@uady.mx, bcruz@uady.mx)*

Abstract: In general, heart medical diagnosis devices are reliable and efficient; however, they are only present in huge or modern hospitals. Heart murmurs are one of the typical heart problems. In this paper, we propose a radial wavelet neural network (RWNN) classifier for cataloging two real heart murmurs (pulmonary insufficiency, PI; and tricuspid insufficiency, TI). The extended Kalman filter (EKF) is used as a learning algorithm for the RWNN. The network inputs are nineteen dimensional features, extracted from real cardiac cycles, and three classification outputs. The proposed model captures the complex nature of the heart cycles more efficiently than a multilayer perceptron trained with Levenberg-Marquardt training algorithm and classifies them accurately. The proposed model is trained and tested using real heart cycles in order to show the applicability of the proposed scheme.

Keywords: wavelets, radial wavelets, neural network, wavelons, heart murmur

1. INTRODUCTION

There are many efficient and reliable heart diagnosis devices. Unfortunately, this modern technology is not available in all hospitals. Cardiac diagnosis is typically started by an auscultation where heart sounds are captured by a stethoscope, from which a medical doctor, depending on his hearing capabilities and training, listens and interprets the acoustic signal. This method of diagnostic is uncertain Watrous et al. (2002), mostly, due to the fact of the human ear loses the acoustic frequency sensitivity through the years B.L.Fishleder (1978). Even though auscultation is not the only way for cardiac diagnosis, it is considered as a primary tool due to its simplicity. Phonocardiography is a technique where heart sounds are registered B.L.Fishleder (1978); this method has an important place as a fortifier of the acoustic interpretation throughout sound graphics (phonocardiogram) from an acoustic-electric transducer. Through a phonocardiogram (PCG), it is possible to analyze the heart acoustic signal from timing, frequency and location point of view and its components in an objective and repetitive form. Heart murmurs are abnormal sounds, which are appreciable in some parts of the vascular system. Neural networks have demonstrated adequate results in PCG's classification Abdel-Motaleb and Akula (2012), Shamsuddin et al. (2005).

Due to their nonlinear modeling characteristics, neural networks have been successfully implemented in control systems, pattern classification and time series forecasting applications. Wavelet transform has been used as signal pre-processor and in neural network classifiers input space feeders Barschdorff et al. (1995), Turkoglu and Arslan (2001); in Gupta et al. (2005), Hadi et al. (2008) up to 90% classification accuracy is achieved. Wavelet neural networks, a combination of wavelet theory and neural networks Veitch (2005), have been used as classifiers in real applications Tian and Gao (2009), Oskouei and Shanbehzadeh (2010). The typical training approach for multilayer perceptrons is the back propagation through time. However, it is a first order gradient descent method, and hence its learning speed could be very slow Leung and Chan (2003). Another well-known training algorithm is the Levenberg-Marquardt one Norgaard et al. (2000); its principal disadvantage is that global minimum is not guaranteed and its learning speed could be slow too, depending on the initialization. In past years, extended Kalman filter (EKF) based algorithm has been introduced to train neural networks Feldkamp et al. (2003). With the EKF based algorithm, the learning convergence is improved Leung and Chan (2003). The EKF training of neural networks, has proven to be reliable for many applications over the past ten years Feldkamp et al. (2003). However, EKF training requires the heuristic selection of some design parameters which is not always an easy task Ricalde et al. (2011).

In this paper we propose a new wavelet neural network (WNN) architecture with EKF training algorithm for classifying heart cycles with murmurs. In order to get the real cardiac sound registers, a monitoring cardiac platform was designed and built. WNN input vectors are amplitude features extracted from segmented cardiac cycles, which (cycles) are obtained via wavelet transform. The applicability of this architecture is illustrated via simulation of the proposed WNN with real heart murmurs in order to show the potential applications for medical cardiac diagnosis devices. The remainder of this paper is organized as follows. Section 2 is dedicated to established medical and mathematical background. Section 3 describes the platform built to acquire and analyzed heart sounds and murmurs. Section 4 and 5 explains the segmentation and feature extraction algorithms performed in order to divide cardiac cycles from PCG's and to extract features from segmented cardiac cycles respectively. Section 6 is dedicated to describe the neural model, where the training phase relies on an extended Kalman filter which is able to deal with the nonlinearity of the model. Section 7 explains methodology used in this research project. Finally, Section 8 reports the experimental analysis of the proposed scheme applied to the problem of classifying real heart murmurs.

2. HEART SOUNDS AND MURMURS

Blood circulation through human body is possible due to the organ that functions as a pump to impulse it: the heart. Heart is compound of 2 separate pumps and four chambers, each side of the heart is compounded of two cavities. Heart has four valves, 2 per side. In the right side we have: aortic and tricuspid valves. In the left side: pulmonary and mitral valves. All the events related from the start of a heartbeat till the beginning of another compose the cardiac cycle. Cardiac cycle (CC) duration varies depending on patient. In a young healthy man, CC duration is 862ms approximately Cabrera Rojo et al. (1997). Heart sounds (HS) are listened by a stethoscope. It is possible to distinguish four HS, but only the first two are sufficient to describe the cardiac valves activity. The first heart sound (S1) is produced by the closure of the mitral and tricuspid valves, the second heart sound (S2) by the closure of the pulmonary and aortic valves. S1 is the first heart sound in the temporal space followed by a S2 and again by a S1. A CC is accomplished with the occurrence of one S1 to another S1 where the HS frequency ranges within 30-600Hz B.L.Fishleder (1978). A microphone within that range is suitable to be employed for the cardiac sounds measurement. The graphical record of the HS is called a phonocardiogram. Heart murmurs are abnormal sounds. When the hole of a valve is squeezed, is called stenosis. When the valve is incompetent to close; this is called insufficiency or regurgitation. Abnormal HS can be watched in a PCG, see Figure 2. From Djebbari and Bereksi Reguig (2000) is known that S1's and S2's frequency range is within 50Hz to 200Hz Ganong (2001).

3. CARDIAC MONITORING PLATFORM

In order to register and capture HS as a PCG, is necessary to have a hardware platform to record them. For this study, a cardiac monitoring platform (CMP) is built. It covers an acoustic-electric (AE) transducer, a signal conditioner (SC) and a USB (Universal Serial Bus) microcontroller. The transducer is composed by a stethoscope coupled with an Electret microphone to register the cardiac sounds and connected to the signal conditioner. The sensor covers the cardiac sounds bandwidth from 30Hz-600Hz B.L.Fishleder (1978). A signal conditioner (SC) is used to amplify the electric signal from sensor (Electret) and as an anti-aliasing filter (4KHz cutoff low pass filter) for the $f_s = 8$KHz sampling frequency chosen. Finally, a USB-microcontroller (uC) is used in order to receive the signal from SC, which is connected to the analog to digital converter (ADC) built-in the uC and send it to computer via USB. In the computer, HS are shown as graphical signals (PCG's) and stored via designed Matlab interface software. CMP is shown in Figure 1. Cardiac registers are stored in the computer to be analyzed.

Every PCG stored by the CMP, has a duration of 15 seconds and is compounded of many CC. Every cardiac cycle has similar behavior about the heart valve where it comes from. It is necessary to make a segmentation of every PCG in single CC in order to perform a medical diagnosis. Cardiac signal, like other biomedical signals, is non-stationary and changes its properties through time. Spectral analysis methods give information about frequency content but they do not involve the time. Continuous time Wavelet transform (CWT) performs time domain analysis on different scales (frequencies), what

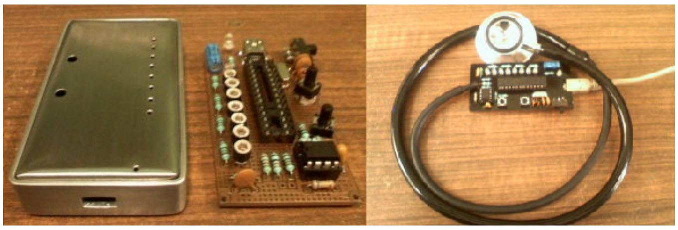

Fig. 1. Cardiac monitoring platform (right); aluminum case and internal board (left)

allows a time space-frequency analysis of a signal. Due to time-frequency analysis and non-stationary behavior of cardiac signal, CWT is frequently used in the analysis of biomedical signals Unser and Aldroubi (1996).

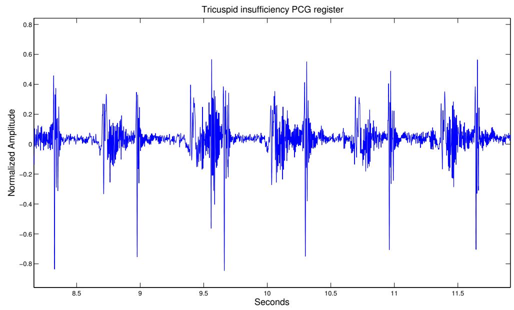

Fig. 2. A tricuspid insufficiency PCG register recorded by CMP

3.1 *Wavelets*

Wavelets are a class of functions used to place a given function in both position and scaling, usually denoted as $\psi(\cdot)$. They are used in applications such as signal processing and time series analysis Veitch (2005).

The continuous time wavelet Transform results(i.e. coefficients) describes the correlation between the signal of interest and the wavelet function through several translations and dilations; these results are called coefficients. For a complete explanation of mathematical criteria about wavelets and continuous time wavelet transform, see Addison (2010). Morlet wavelet is the wavelet function that better supplies frequency-time location for the analysis of biomedical signals Unser and Aldroubi (1996).

4. SEGMENTATION

Once a cardiac register is acquired, CWT is applied with the Morlet wavelet and a three dimensional graphic is obtained for the discrete time acquired data, scales and coefficients. The scale can be switched by frequencies through the following equation:

$$f = \frac{f_0}{aT_s} \tag{1}$$

See Addison (2010) for details. Where f_0 is the central frequency of the wavelet (i.e. The frequency where the module of the Fourier transform of the wavelet signal is maximum) and $T_s = 1/f_s$. The continuous wavelet transform $\mathbf{W}_{a,b} \in \Re^{f_1 \ x \ t_1}$ computation is performed over the intervals $a \in [a', f_1]$ (i.e. $a's$ values that can be transformed to frequency units with equation (1), that were computed) and $b \in [T_s, t_1]$ (i.e. set of step samples in the 15s record length of every PCG; from T_s, as first value, to t_1), where f_1(scale value) represents the maximum scale value(frequency) chosen to be computed; $t_1 = 15s * f_s = 15s * 8000\frac{samples}{s} = 120,000\ samples$, fixed max number of discrete time data; $a' \in \Re^{+}$. In order to find S1's from a PCG, $\mathbf{W}_{(a,b)}$ is computed with $a \in (0, 200]$ and $b \in [T_s,\ t_1]$, a coefficient matrix $T \subset \mathbf{W}_{a,b}$ is extracted from row 33 to 65 (100Hz to 196Hz) of $\mathbf{W}_{a,b}$ what can be noticed in Figure 3. Now, the half maximum energy value of $\mathbf{W}_{(a,b)}$ is taken as reference (ref). Then, we go through $\mathbf{T}$, column by column, evaluating the function $f(u)$ for each value $T_{i,j}$ as

$$f(u) = \begin{cases} 0 \ if \ u < ref \\ u \ if \ u \geq ref \end{cases} \tag{2}$$

These results are stored in $\mathbf{M} \in \Re^{f_1\ x\ t_1}$. Then a row vector $\boldsymbol{busq}$ is generated by the maximum values of all the columns of $\mathbf{M}$. Where $\boldsymbol{busq}$ is described by:

$$\boldsymbol{busq} = max(col_{\mathbf{M}}(i)) \ \ for \ i = 1, 2, 3, \ldots, 120,000 \tag{3}$$

where $col_{\mathbf{M}}(i)$ describes the ith column vector of matrix $\mathbf{M}$. The tones S1 and S2 are within $\mathbf{M}$ and is necessary to identify them from it. The tone S1 is expected to have three ideal characteristic maximum amplitude components and the S2 tone, two B.L.Fishleder (1978). Even when in practice is difficult to find these 3 components for S1, more amplitude oscillations in PCG's are found in the S1. This fact is used in order to distinguish S1 from S2 within $\mathbf{M}$. A second treatment is performed as follows: $\boldsymbol{busq}$ is now composed of zeros and values upon $ref/2$ (different than zero). Inside $\boldsymbol{busq}$, we proceed to navigate through the generated zeros, looking for a value different than zero. Once it is found, n the number of changes from a value different of zero to zero and vice versa are analyzed in order identify a S1 tone. If a second heart sound would have been in the search inside $\boldsymbol{busq}$ with m changes, about the three ideal amplitude components of S1's, it is expected to obtain $n > m$ or in the worst case, to have $n = m$ B.L.Fishleder (1978). In this work, $n = 4$ is taken, since at least two amplitude components are expected to appear in S1, which represents four changes. Now, we take x as the changes discovered in the finding process. A third treatment is performed as follows: we delimit the beginning of an interval of a possible S1 with the finding of a value different than zero within $\boldsymbol{busq}$. Once $x > n$, a reference of $l = 1200\ zeros$ are counted in order to delimit the end of a S1. More changes can be found, but till l zeros are reached, interval is closed and stored as a S1. l represents 150ms with $t_s = 125\mu s$, it is a little more than one octave of the average of CC duration in young healthy man (862ms) Cabrera Rojo et al. (1997), that avoids to take a finding interval too long including more outcomes (i.e. possible S2's or signal oscillations due to patient movements). l is also used to discard any invalid S1 interval. Once $x > 0$, l starts to count. If $x > n$ is not satisfied and l reaches 1200 zeros, a possible S1 interval is rejected. In order to find S2, the outcomes of the S1 are used in the time domain of the PCG. From a pair of S1 tones, $t = l = 150ms$ milliseconds are shifted to the center, among this interval of time, the maximum value is stored as a S2. This algorithm is used for all existence pairs in the PCG and applied for no murmur, tricuspid and pulmonary insufficiency PCG's.

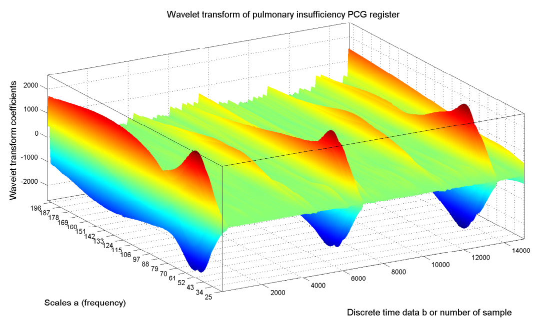

Fig. 3. Wavelet transform plot of pulmonary insufficiency PCG register

5. FEATURE EXTRACTION

Now, that we have segmented PCG's, a feature extraction of the shape of the signal is performed. Feature extraction values are extracted from the S1-S2 process, called systole; and from S2-S1 process, called diastole. Cardiac cycle duration varies from cycle to cycle in the same patient and from patient to patient. Then, a feature extraction algorithm independently of the cycle duration is necessary. It must be also capable of modeling amplitude shape of the murmurs to be delivered to the neural network. To reach this goal, an algorithm of middle relative divisions made recursively upon each division generated on a symmetric way is performed, taking previous S1's and S2's outcomes. A S1 and S2 is taken, a middle time division is made among them. Time divisions intervals created by the first one are divided again symmetrically and so on. Nine divisions are taken in this way. Extreme borders divisions are taken from S1's and S2's outcomes and translated $t = l = 150ms$ milliseconds to the center, to ensure S1's and S2's oscillations have been left behind. Upon each division, a feature can be extracted. All points chosen are used as neural network inputs. However, to maximize feature extraction performance, a time neighborhood ε is taken and the maximum amplitude value between this vicinity is chosen as feature. A minimum amplitude feature in each division is taken as well, to better model murmurs oscillations. In addition, a small μ amplitude interval is selected to qualify if a feature must be cleared to zero, in order to benefit neural network effectiveness. PCG's registers are normalized in the closed interval of $[-1, 1]$, $\mu = [-0.05, 0.05]$ and vicinity ε = 12.5ms are taken. 9 points for minimum and 9 for maximum values at divisions are taken. It represents a total of 18 features (9 maximum and 9 minimum) from diastole and 18 features for systole of every CC and of all PCG's registered. Systole or diastole features are used depending on heart murmur disease. In Figure 4, features extracted from several heart murmurs PCG's are shown.

6. PROPOSED MODEL

A Neural network (NN) is trained to learn an input-output map. Theoretical works have proven that, even with just one hidden layer, a NN can uniformly approximate any continuous function over a compact domain, provided that the NN has a sufficient number of synaptic connections Alanis et al. (2010).

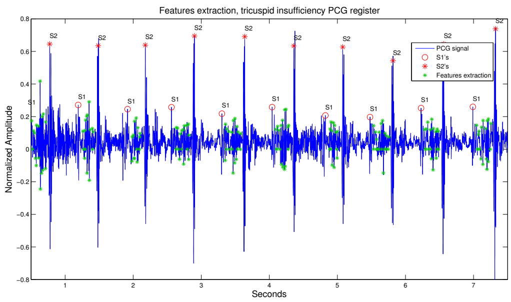

Fig. 4. Segmented tricuspid insufficiency PCG register with features extracted marked

6.1 *WNN*

A wavelet neural network generally consists of a feed-forward neural network, with one hidden layer, whose activation functions are taken from a wavelet family.

Radial Wavelets A wavelet function φ , to be considered as radial, has to have the form

$$\varphi(x) = \phi(\|x\|) \tag{4}$$

where $\|x\| = \left(x^T x\right)^{\frac{1}{2}}, x \in \Re^n, \phi : \Re \to \Re$ is a univariable function. A neuron which activation fuction is a wavelet is called a wavelon. Radial multidimensional wavelons (RMW) have the following computational complexity: the computation of $\varphi(x)$ requires, the norm of x and the evaluation in the univariable function ϕ. This complexity is comparable with the multidimensional wavelets of inner product shown in Zhang and Benveniste (1992). RMW are introduced in Zhang (1992) and are different than the shown in Zhang and Benveniste (1992). In Borowa A. (2007) RMW characteristics are exposed that make them to be consider as better choice than the processing units shown in Zhang and Benveniste (1992).

6.2 *The EKF learning algorithm*

The Kalman filter (KF) estimates the state of a linear system with state and output additive white noises Sanchez Camperos and García Alanís (2006), Chui and Chen (2009), Song and Grizzle (1992). For KF-based neural network training, the network weights become the states to be estimated. In this case the error between the neural network output and the measured plant output can be considered as the additive white noise Haykin (2001). Although the white noise assumption is not satisfied, the algorithm has been efficient in real applications. Due to the fact that the neural network mapping is nonlinear, an EKF type is required Sanchez et al. (2004), Sanchez Camperos and García Alanís (2006). The training goal is to find the weight values which minimize the prediction error. EKF learning algorithm is described by

$$\hat{w}(k+1) = \hat{w}(k) + n_K K(k)\left[y(k) - \hat{w}(k)\right] \tag{5}$$

$$K(k) = P(k) H^T(k)\left[R(k) + H(k) P(k) H^T(k)\right]^{-1} \tag{6}$$

$$e(k) = y(k) - \hat{y}(k) \tag{7}$$

$$P(k+1) = P(k) - K(k) H(k) P(k) + Q \tag{8}$$

where $e(k) \in \Re$ is the output estimation error, $P(k) \in \Re^{N\ x\ N}$ is the weight estimation error covariance matrix at step k, $w(k) \in \Re^{\mathrm{N}}$ is the weight (state) vector, N is the respective number of neural network weights, $y(k) \in \Re^S$ is the plant output, where S is the number of outputs; $\hat{y}(k)$ is the NN output, $K \in \Re^{N\ x\ S}$ is the Kalman gain, $Q \in \Re^{\mathrm{NxN}}$ is the NN weight estimation noise covariance matrix, $0 < n_K < 1$ is the learning coefficient, $R \in \Re^{\mathrm{SxS}}$ is the error noise covariance. $H \in \Re^{\mathrm{SxN}}$ is a matrix, in which each output ($\hat{y}_i$), is derivative with respect of each weight (w_j), defined as follows:

$$H_{ij}(k) = \left[\frac{\partial \hat{y}_i(k)}{\partial w_j(k)}\right]^T_{w(k)\,=\,\hat{w}(k+1)} \tag{9}$$

where $i = 1, \ldots, S$ and $j = 1, \ldots, N$. Usually P, Q y R are initialized as diagonal matrices, with initial entries $P(0)$, $Q(0)$ y $R(0)$ respectively. Additionally H, K and P for the EKF are bounded; for a explanation of this fact, see Song and Grizzle (1992).

6.3 *Proposed RWNN classifier*

The proposed RWNN has the potential to detect several cardiac anomalies depending on the registered data. The RWNN has an entry layer, one hidden wavelon layer and a linear output layer with sigmoid functions. The sigmoid output functions images are defined within the interval $(-1, 1) \in \Re$.

The RWNN has 19 connections to the hidden layer (through the weight matrix **W1**). The outputs from the hidden layer are connected (through the weight matrix **W2**) to the output linear layer and finally passed through sigmoid functions.

The first 18 input values are extracted as amplitude features from every cardiac cycle. The nineteenth input is a fixed value, from the auscultation focus source of the cardiac cycle (pulmonary, 0.1; tricuspid, 0.2 and no murmur PCG, 0). The neural outputs are 3: no murmurs (NM) first, the second correspond to PI and the last one to TI. Criteria of the RWNN outputs (i.e. due to possible infinite values in the sigmoid function image) is chosen as three zones: high, low or uncertain. This criteria is defined as $0 < low < 0.25$, $0.25 < uncertain < 0.85$, $0.85 < high < 1$. The main task of the RWNN is to obtain a *high* in the correct neural network output and *low* in the left ones; if this happens, we considered the cycle as *acceptable* (A), if not, an *error* (Err). We consider a *false negative* (FN) when outputs that must be cleared reach *low* (i.e. what is correct), for a given cycle, but net says *low* instead of *high*, in the proper output. False positives do not apply in this research due to the absence of PCG's registers with diseases different than PI and TI and the definition of an Err. An *uncertain* (U) CC is considered if wrong outputs reach *low* (i.e. what is correct) and the correct one remains on the *uncertain* zone instead of *high*. The RWNN shown in Fig 5 is described by

$$x_j = \left[\sum_{i=1}^{n} (u_i \omega_{ij})^2\right]^{\frac{1}{2}} \tag{10}$$

$$\begin{aligned}\varphi_j\left((x_j - b_j)/a_j\right) = &\left(n_a - \left((x_j - b_j)/a_j\right)^2\right) \\ &\cdot exp\left(-\left((x_j - b_j)/a_j\right)^2/2\right)\end{aligned} \tag{11}$$

$$v_k = \sum_{j=1}^{m} \varphi_j\left((x_j - b_j)/a_j\right)\omega_{jk} + \bar{y}_k \tag{12}$$

$$y_k = 1/\left(1 + exp(-a_s v_k)\right) \tag{13}$$

where $n =$ is the number of inputs from the feature extraction algorithm (19 inputs), $m =$ is the number of wavelons in the hidden layer, $k =$ number of outputs, $a_s =$ sigmoid slope parameter, $\bar{y}_k =$ the bias parameters, w_{ij} is the $ijth$ element of $\mathbf{W}_1$ and w_{jk} the $jkth$ element of $\mathbf{W}_2$, $dim(\mathbf{W}_1) = 19 \times m, dim(\mathbf{W}_2) = m \times k$, $dim(\mathbf{W}) = dim(\mathbf{W_1}) + dim(\mathbf{W_2}) + k = (19 \times m) + (m \times 3) + 3$. φ_j is the radial wavelet activation function for the jth wavelon, called, *mexican hat radial wavelet*. Each φ_j wavelet has its own b_j and a_j parameters that represent translation and dilation parameters for the jth wavelon, respectively. φ_j also has n_a as a scaled parameter of the wavelet. Parameters are initialized as follows: a $L \in \Re^+$ is taken, $a's$ are set to 2^L and $b's$ to 2^{-L}, **W1** and **W2** at 0.1. $L = 0.5$ and $a_s = 0.6$, $n_a = 10$ are taken. $b's$ and $a's$ in each wavelon are not modified by learning algorithm during training. $\bar{y}_k$ bias parameters are initialized as the average of all the available observations (desire target outputs) and are involved as weights in EKF learning algorithm. Only **W1** and **W2** are modified by EKF learning algorithm. Initialization of **W1**, **W2**, $b's$, $a's$, and $\bar{y}_k$ are based on wavelet networks theory Veitch (2005); Zhang and Benveniste (1992) with adjustments on weights and L value. EKF learning algorithm parameters are initialized on identity matrices for simplicity, scaled with scalar values, where scaled values satisfied $\varepsilon_m = (0, 3] \in \Re$ and satisfied $P(0) > R(0) > Q(0)$. $P(0)$, $Q(0)$, $R(0)$, n_a, n_K and a_s are heuristically determined. Implemented RWNN is shown in Figure 5.

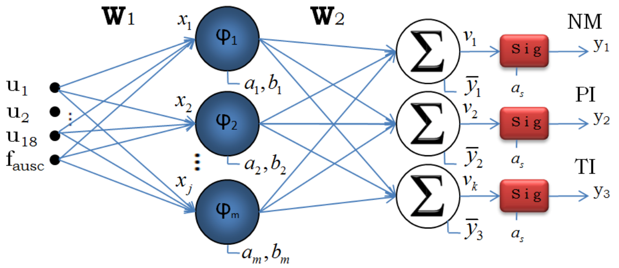

Fig. 5. Proposed RWNN

where f_{ausc} denotes the nineteenth input and is related to the auscultation focus source, mentioned before. sig is the sigmoid function in (13) with slope parameter a_s.

7. METHODOLOGY

As first step, real PCG's with murmurs are registered from patients with the CMP (109 cardiac cycles acquired). For the registered data with the CMP, the continuous time wavelet transform is applied for analysis via software, as part of the segmentation stage. Then, the feature extraction algorithm is applied and features for every cardiac cycle are computed. Some cardiac cycles are selected to train the neural network, and the remaining of the data is used to test the neural network performance. See next section for more details.

8. EXPERIMENTAL RESULTS

The RWNN is trained by EKF with 17 training examples, 9 PI, 5 TI and 3 NM; and tested with 92 cardiac cycles, 38 PI (first cycles) and 54 TI cycles. Which represents a collection of 109 real cardiac cycles acquired with the CMP. Mean square error (MSE) is used as a performance measure for every output. See Ricalde et al. (2011) for MSE function description.

RWNN performance is compared with a multilayer perceptron (MLP) structure with an exact parallel architecture. MLP structure is shown in Figure 6. Where b_{j1} and b_{k2} are bias parameters. Linear functions on neurons are displayed as diagonal lines and *tansig* refers to sigmoid functions of image $[-1, 1] \in \Re$. This structure is trained with Levenberg-Marquardt (L-M) learning algorithm initialized in $\mu = 0.1$, μ .inc = 8, μ .dec = 0.1. Where μ is a scalar parameter, $\mu.inc$ and $\mu.dec$ increase and decrease factors, respectively. Levenberg-Marquardt learning algorithm and neural network functions such as activation and output functions, are used for comparison. Training and performance results for networks are shown in Table 1 and Table 2, respectively. Where $Epochs$, are the number of times training data (cardiac features from cardiac cycles) are submitted to the RWNN in order improve the learning through EKF-training.

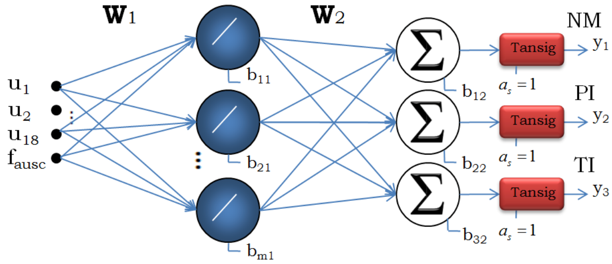

Fig. 6. Neural network structure for comparing

Table 1. Training results

	RWNN	MLP
Learning	EKF	L-M
Weights	223	233
Wavelons/Neurons	10	10
Epochs	90	12
MSE (Outputs average)	$4.6355e^{-6}$	$8.63e^{-9}$

Table 2. Performance results

	RWNN	MLP
Learning	EKF	L-M
Acceptable	89	70
Uncertainty	0	4
Errors	2	18
False negatives	1	0
Accuracy	96.74%	76.08%

9. CONCLUSION

This paper proposes the use of a RWNN trained with EKF learning algorithm, to classify segmented real heart murmurs cycles. Experimental results showed that the proposed RWNN is very well suited for classification of real PCG's segmented cycles as shown in Table 2. Even when neural network trained with Levenberg-Marquardt used for comparison (See Figure 6 and Table 1) was significantly better at training, adjusting weights for converging at lower output error in less epochs (12 epochs) than RWNN, it presented superior generalization capabilities. Future work on implementing RWNN aims to be in the development of reliable medical heart instrumentation.

ACKNOWLEDGEMENTS

Authors want to thank Medic M.S. Rafael Eduardo Aguilar Romero for his participation on medical documentation and medic Addy Castillo Espinola for giving us the opportunity of acquiring PCG's registers in T1 IMSS hospital, Mérida, Yucatán, México. To Sansore's family for helping on cardiac monitoring platform.

REFERENCES

Abdel-Motaleb, I. and Akula, R. (2012). Artificial intelligence algorithm for heart disease diagnosis using phonocardiogram signals. In *Electro/Information Technology (EIT), 2012 IEEE International Conference on*, 1 –6. doi: 10.1109/EIT.2012.6220714.

Addison, P. (2010). *The Illustrated Wavelet Transform Handbook: Introductory Theory and Applications in Science, Engineering, Medicine and Finance*. Taylor & Francis.

Alanis, A.Y., Sanchez, E.N., and Ricalde, L.J. (2010). Discrete-time reduced order neural observers for uncertain nonlinear systems. *Int. J. Neural Syst.*, 20(1), 29–38.

Barschdorff, D., Femmer, U., and Trowitzsch, E. (1995). Automatic phonocardiogram signal analysis in infants based on wavelet transforms and artificial neural networks. In *Computers in Cardiology 1995*, 753 –756. doi: 10.1109/CIC.1995.482774.

B.L.Fishleder (1978). *Exploración Cardiovascular y Fonomecanocardiografía Clínica*. La Prensa Mexicana.

Borowa A., Brdys M.A., M.K. (2007). Modelling of wastewater treatment plant for monitoring and control purposes by state – space wavelet networks. *International Journal of Computers Communications & Control*, 2(2), 121–131.

Cabrera Rojo, I., Cabrera Santos, A., and Gallardo Montes de Oca, G. (1997). Variabilidad de la frecuencia cardíaca en el joven normal. *Revista Cubana Investigación Biomédica*, 16(2), 98–103.

Chui, C.K. and Chen, G. (2009). *Kalman Filtering with Real-Time Applications*, volume 17 of *Springer Series in Information Sciences*. 4th edition.

Djebbari, A. and Bereksi Reguig, F. (2000). Short-time fourier transform analysis of the phonocardiogram signal. In *Electronics, Circuits and Systems, 2000. ICECS 2000. The 7th IEEE International Conference on*, volume 2, 844–847. doi: 10.1109/ICECS.2000.913008.

Feldkamp, L.A., Prokhorov, D.V., and Feldkamp, T.M. (2003). Simple and conditioned adaptive behavior from Kalman filter trained recurrent networks. *Neural Networks*, 16(5-6), 683 – 689. doi:http://dx.doi.org/10.1016/S0893-6080(03)00127-8.

Ganong, W. (2001). *Fisiología Médica*. Manual Moderno, México, 20th edition.

Gupta, C.N., Palaniappan, R., and Swaminathan, S. (2005). Classification of homomorphic segmented phonocardiogram signals using grow and learn network. In *Engineering in Medicine and Biology Society, 2005. IEEE-EMBS 2005. 27th Annual International Conference of the*, 4251–4254. doi: 10.1109/IEMBS.2005.1615403.

Hadi, H., Mashor, M., Mohamed, M., and Tat, K. (2008). Classification of heart sounds using wavelets and neural networks. In *Electrical Engineering, Computing Science and Automatic Control, 2008. CCE 2008. 5th International Conference on*, 177 –180. doi:10.1109/ICEEE.2008.4723403.

Haykin, S. (2001). *Kalman Filtering and Neural Networks*. John Wiley and Sons, New York, USA.

Leung, C.S. and Chan, L.W. (2003). Dual extended Kalman filtering in recurrent neural networks. *Neural Networks*, 16(2), 223 – 239. doi:10.1016/S0893-6080(02)00230-7.

Norgaard, M., Poulsen, N.K., and Ravn, O. (2000). Advances in derivative- free state estimation for nonlinear systems. Technical report immrep-1988-15, Technical University of Denmark.

Oskouei, B. and Shanbehzadeh, J. (2010). Chromosome classification based on wavelet neural network. In *Digital Image Computing: Techniques and Applications (DICTA), 2010 International Conference on*, 605 –610. doi: 10.1109/DICTA.2010.107.

Ricalde, L., Catzin, G., Alanis, A., and Sanchez, E. (2011). Higher order wavelet neural networks with Kalman learning for wind speed forecasting. In *Computational Intelligence Applications In Smart Grid (CIASG), 2011 IEEE Symposium on*, 1–6. doi:10.1109/CIASG.2011.5953332.

Sanchez, E.N., Alanis, A., and Chen, G. (2004). Recurrent neural networks trained with Kalman filtering for discrete chaos reconstruction. In *Proceedings of Asian-Pacific Workshop on Chaos Control and Synchronization*. Melbourne, Australia.

Sanchez Camperos, E.N. and García Alanís, A.Y. (2006). *Redes neuronales: conceptos fundamentales y aplicaciones a control automático*. Automática y robótica. Pearson Educación.

Shamsuddin, N., Mustafa, M., Husin, S., and Taib, M. (2005). Classification of heart sounds using a multilayer feed-forward neural network. In *Sensors and the International Conference on new Techniques in Pharmaceutical and Biomedical Research, 2005 Asian Conference on*, 87 – 90. doi:10.1109/ASENSE.2005.1564512.

Song, Y. and Grizzle, J.W. (1992). The extended Kalman filter as a local asymptotic observer for nonlinear discrete-time systems. In *American Control Conference, 1992*, 3365–3369.

Tian, J. and Gao, M. (2009). Research of web classification mining based on wavelet neural network. In *Artificial Intelligence, 2009. JCAI '09. International Joint Conference on*, 559 –562. doi:10.1109/JCAI.2009.209.

Turkoglu, I. and Arslan, A. (2001). An intelligent pattern recognition system based on neural network and wavelet decomposition for interpretation of heart sounds. In *Engineering in Medicine and Biology Society, 2001. Proceedings of the 23rd Annual International Conference of the IEEE*, volume 2, 1747 – 1750. doi:10.1109/IEMBS.2001.1020555.

Unser, M. and Aldroubi, A. (1996). A review of wavelets in biomedical applications. *Proceedings of the IEEE*, 84(4), 626–638. doi:10.1109/5.488704.

Veitch, D. (2005). *Wavelet neural networks and their application in the study of dynamical systems*. M.s. thesis, Department of Mathematics, University of York, United Kingdom.

Watrous, R., Grove, D., and Bowen, D. (2002). Methods and results in characterizing electronic stethoscopes. In *Computers in Cardiology, 2002*, 653 – 656. doi: 10.1109/CIC.2002.1166857.

Zhang, Q. and Benveniste, A. (1992). Wavelet networks. *Neural Networks, IEEE Transactions on*, 3(6), 889 –898. doi: 10.1109/72.165591.

Zhang, Q. (1992). Wavelet network : The radial structure and an efficient initialization procedure. Technical Report 1423, Linköping University, The Institute of Technology.